

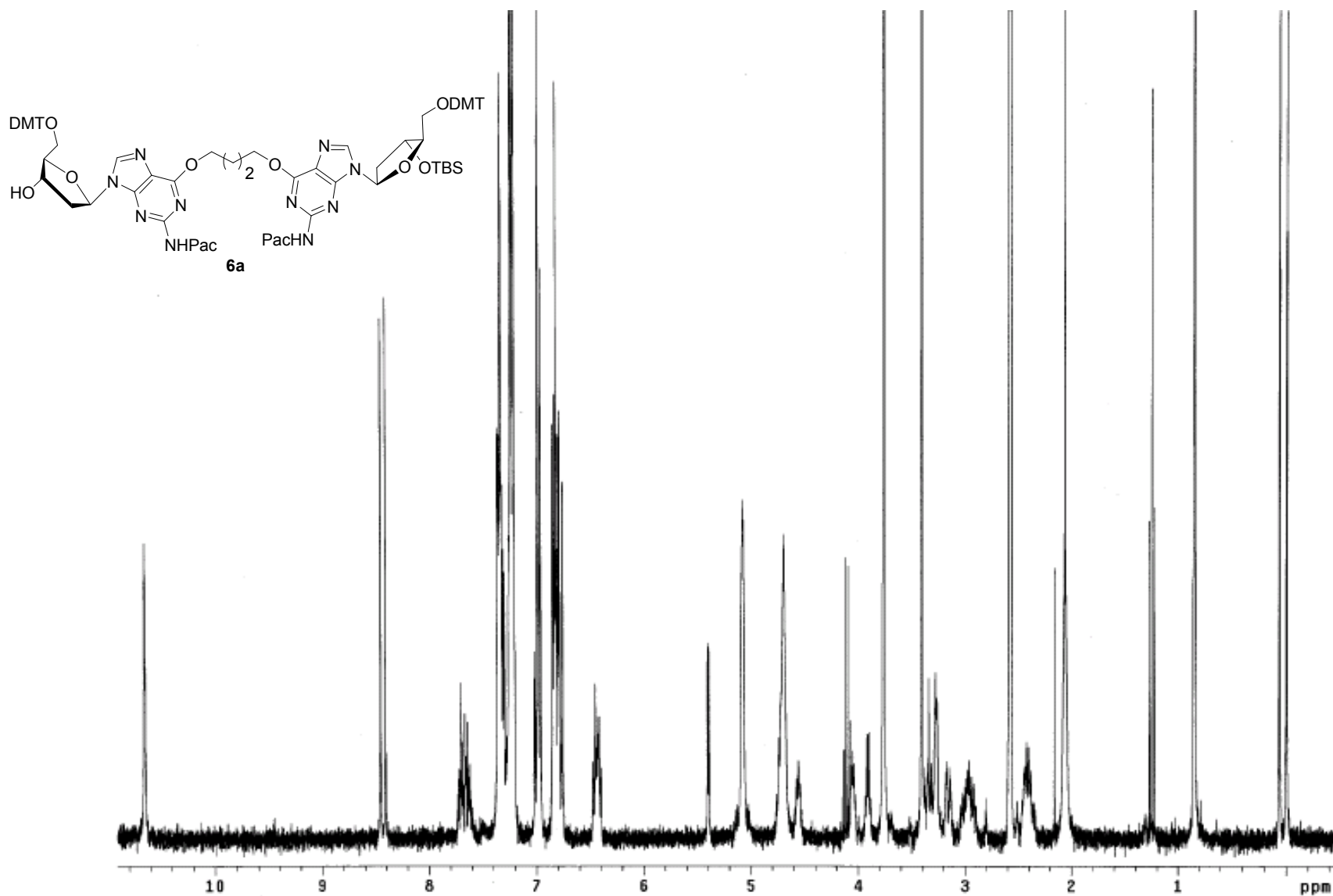
Electronic Supplementary Information

Synthesis and Characterization of Oligonucleotides Containing an O⁶-2'-Deoxyguanosine-Alkyl-O⁶-2'-Deoxyguanosine Interstrand Cross-Link in a 5'-GNC Motif and Repair by Human O⁶-Alkylguanine-DNA Alkyltransferase

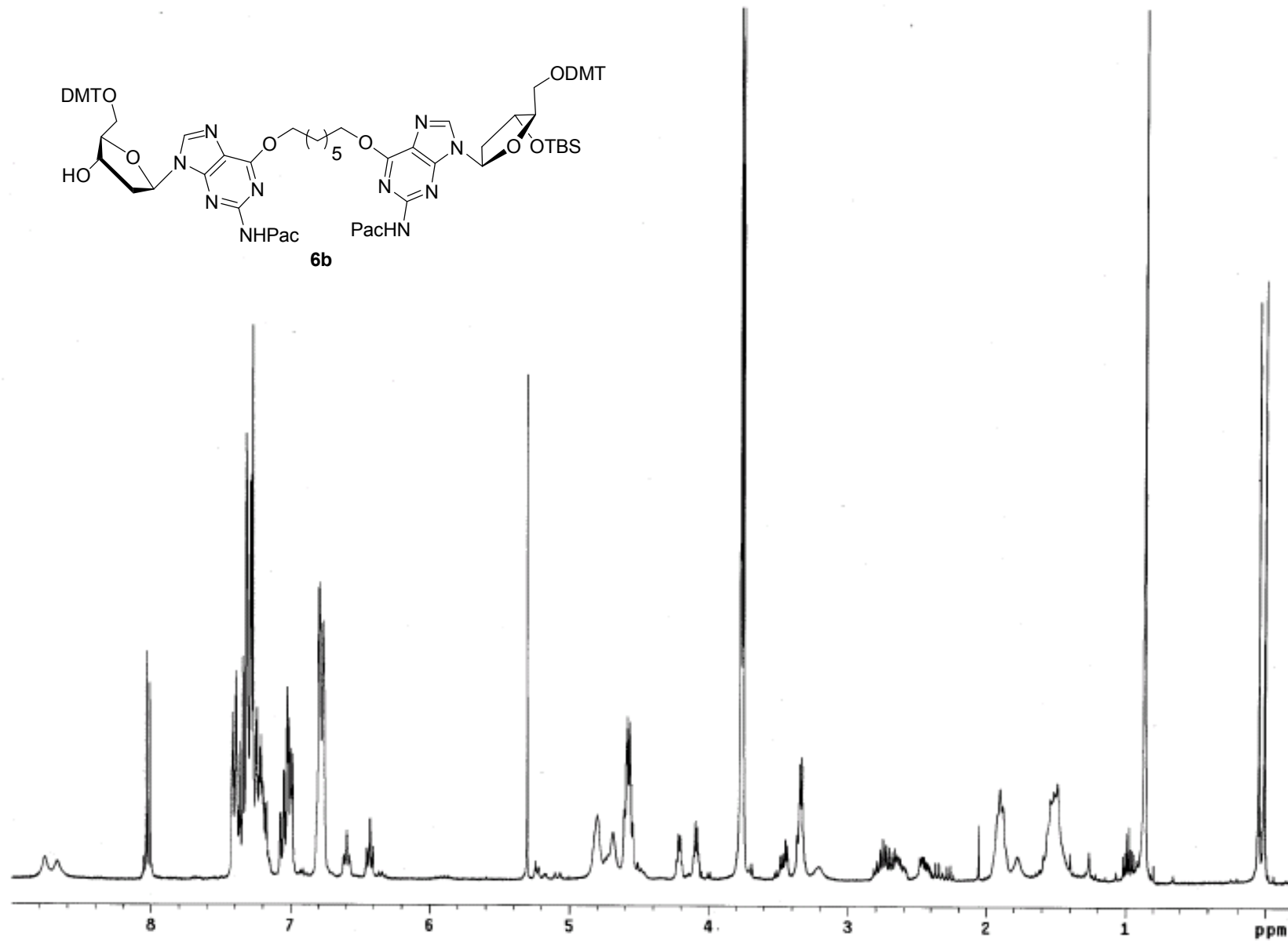
Francis P. McManus, Qingming Fang, Jason D. M. Booth, Anne M. Noronha, Anthony E. Pegg and Christopher J. Wilds*

Contents	Page
Supplementary Figure 1 - 300 MHz ¹ H NMR spectrum of compound (6a) (in d ₆ -DMSO)	S-2
Supplementary Figure 2 - 300 MHz ¹ H NMR spectrum of compound (6b) (in CDCl ₃)	S-3
Supplementary Figure 3 - 121.5 MHz ³¹ P NMR spectrum of compound (7a) (in d ₆ -acetone)	S-4
Supplementary Figure 4 - 121.5 MHz ³¹ P NMR spectrum of compound (7b) (in d ₆ -acetone)	S-5
Supplementary Figure 5 - C-18 RP HPLC profiles to monitor TBS removal	S-6
Supplementary Figure 6 - Strong anion exchange HPLC profiles of crude and purified XL7	S-7
Supplementary Figure 7 - C-18 RP HPLC profile of digested cross-linked duplexes XL4 and XL7	S-8
Supplementary Figure 8 - ESI MS spectrum of oligonucleotide XL4	S-9
Supplementary Figure 9 - ESI MS spectrum of oligonucleotide XL7	S-10
Supplementary Figure 10 - Absorbance (A ₂₆₀) versus temperature profiles	S-11
Supplementary Figure 11 - CD spectra of non cross-linked control duplex and cross-linked duplexes XL4 and XL7	S-12
Supplementary Figure 12 - Molecular models of non cross-linked control duplex and cross-linked duplexes XL4 and XL7	S-13
Supplementary Figure 13 - 12% SDS-PAGE Gel of purified hAGT proteins	S-14
Supplementary Figure 14 - Effects of mutations on secondary structure of hAGT by CD	S-15
Supplementary Figure 15 - Effects of mutations tertiary structure of hAGT by monitoring intrinsic fluorescence	S-16
Supplementary Figure 16 - Effect of mutations on hAGT stability monitored by thermal denaturation as measured by CD	S-17
Supplementary Figure 17 - Graphic representation of the % ICL	S-18
Supplementary Figure 18 - Time course repair of XL4 and XL7 by hAGT	S-19
Supplementary Figure 19 - Graphic representation of the % abundance of each species in the time course repair by hAGT	S-20
Supplementary Figure 20 - Electromobility shift assay of C145S hAGT binding to the control DNA duplex	S-21
Supplementary Figure 21 - Hill plot representation of log[PD]/[D] versus log[P] for the control duplex	S-22
Supplementary Table 1 - ESI-MS results of wild-type hAGT and variants	S-23
Supplementary Table 2 - Effects of mutations on fluorescence emission signals of hAGT	S-24
Supplementary Table 3 - Difference in <i>T_m</i> between mutants and wild-type hAGT	S-25

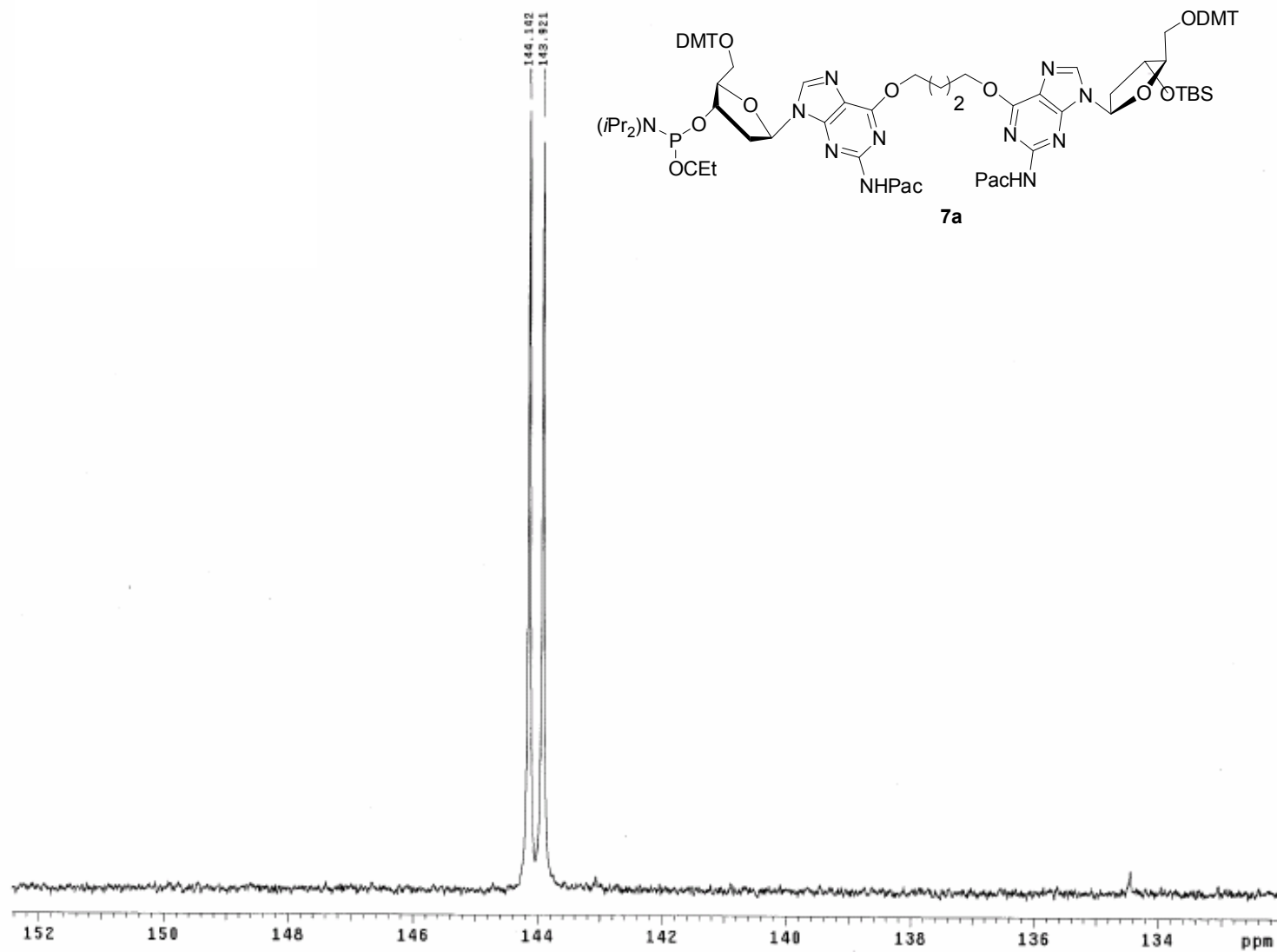
Supplementary Figure 1 - 300 MHz ^1H NMR spectrum of compound (**6a**) (in $\text{d}_6\text{-DMSO}$)



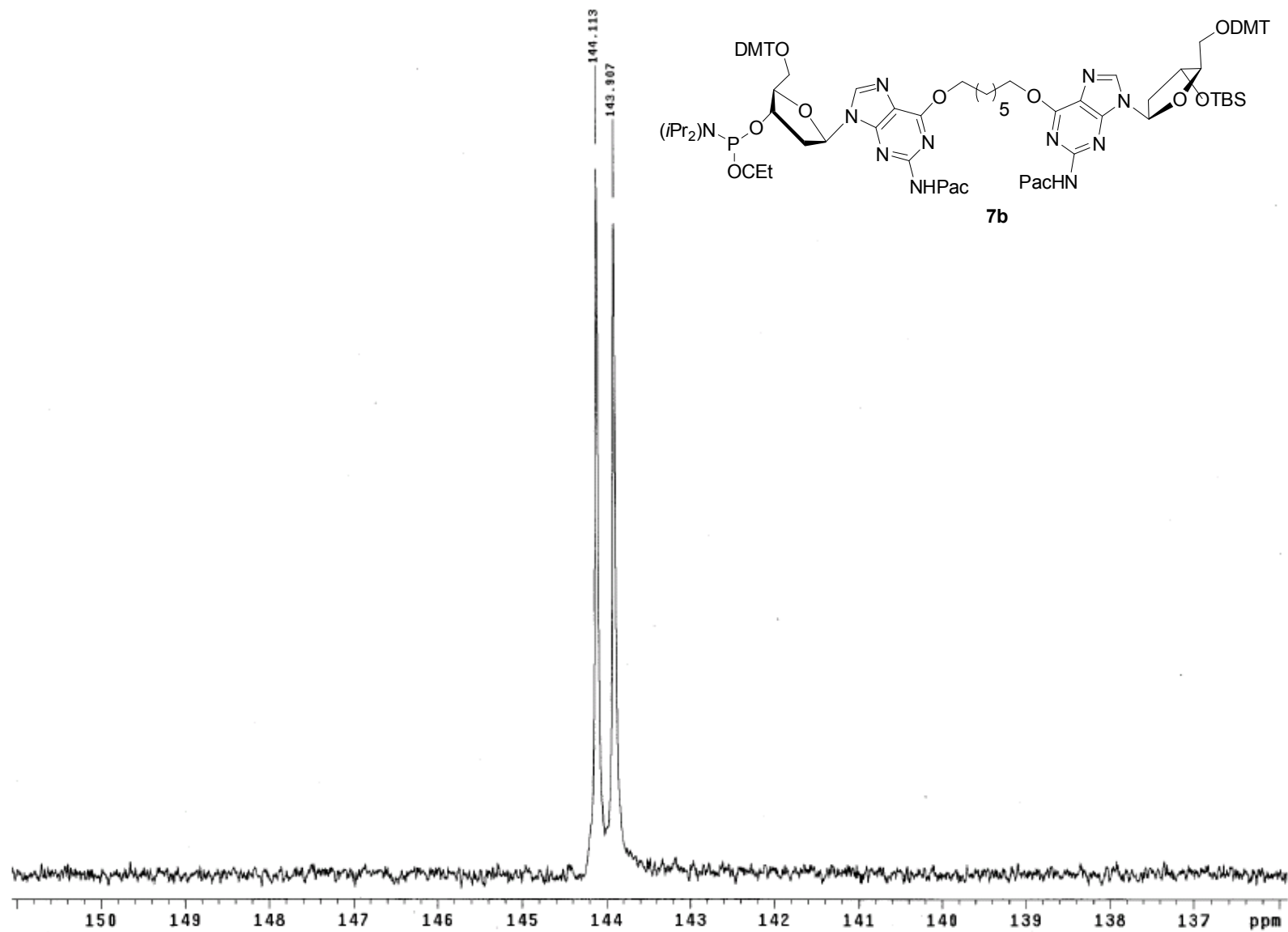
Supplementary Figure 2 - 300 MHz ^1H NMR spectrum of compound (**6b**) (in CDCl_3)



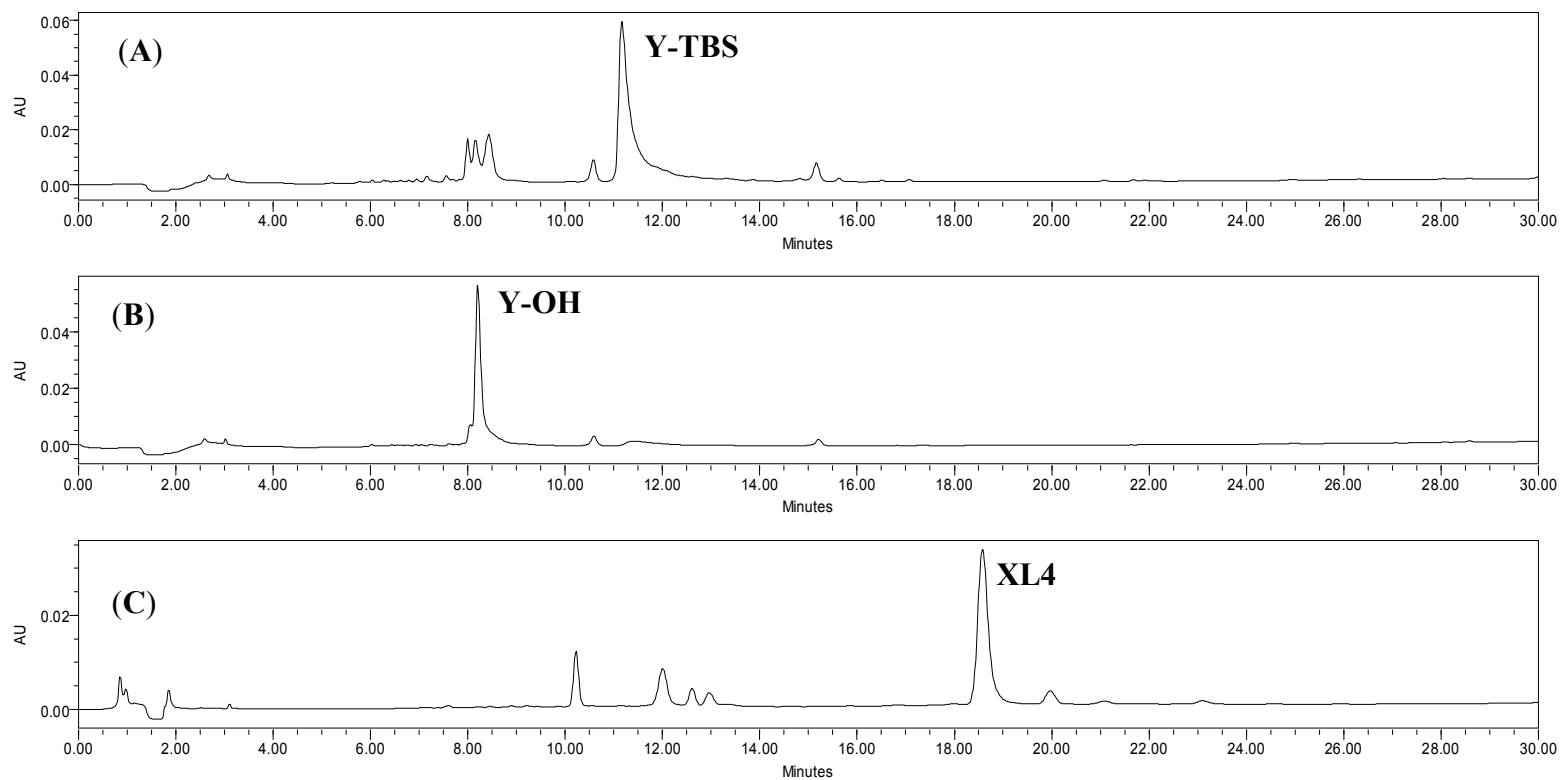
Supplementary Figure 3 - 121.5 MHz ^{31}P NMR spectrum of compound (**7a**) (in d_6 -acetone)



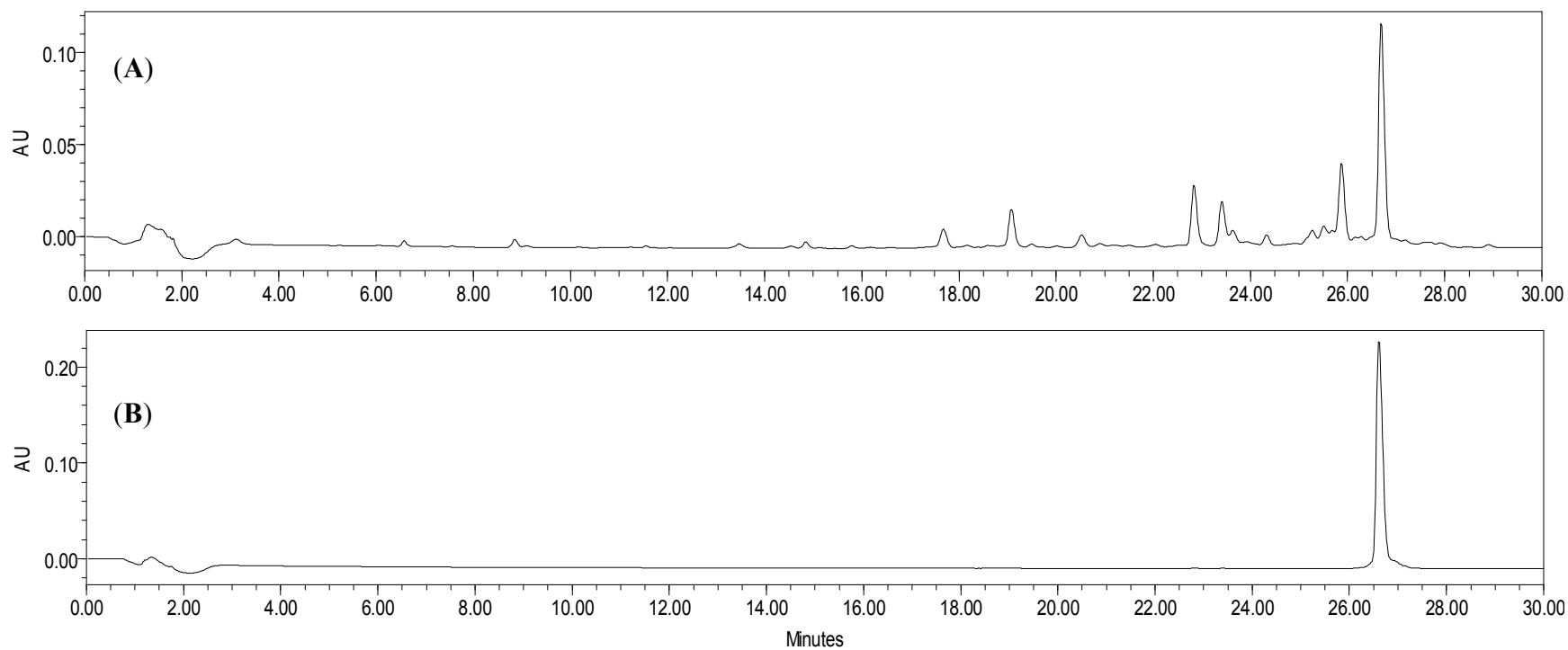
Supplementary Figure 4 - 121.5 MHz ^{31}P NMR spectrum of compound (**7b**) (in d_6 -acetone)



Supplementary Figure 5 - C-18 HPLC profiles of (A) crude **Y-TBS** (**XL4** precursor), (B) **Y-OH** after removal of the TBS group, and (C) final extension product **XL4**. Gradient of 0-60% buffer B over 30 min (buffer A: 50 mM sodium phosphate, pH 5.8 and buffer B: 50 mM sodium phosphate, pH 5.8, 50% acetonitrile) at a flow rate of 1.0 mL/min and monitored at 260 nm.

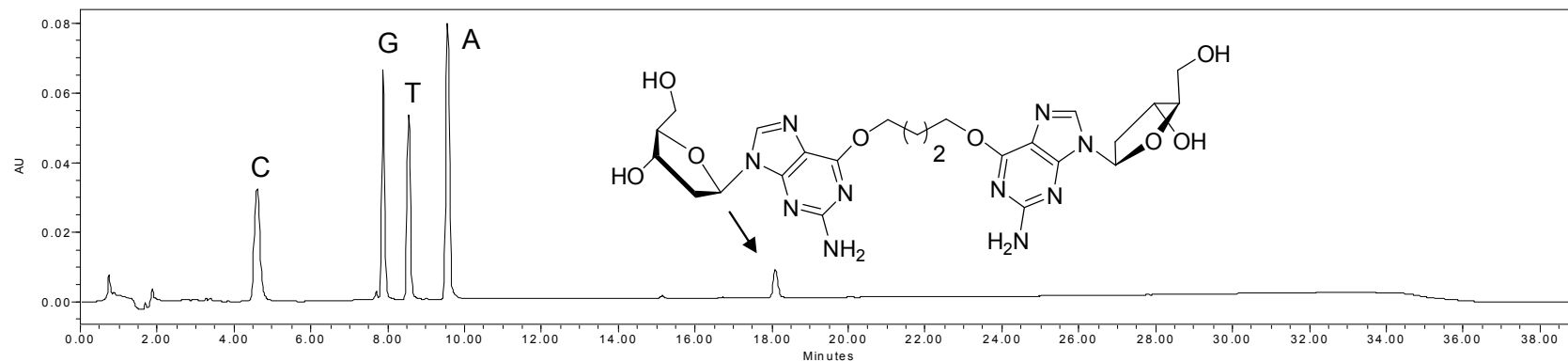


Supplementary Figure 6 - SAX HPLC profiles of crude **XL7** (A) and purified **XL7** (B). For analytical runs the column was eluted with a linear gradient of 0-60% buffer B over 30 min (buffer A: 100 mM Tris HCl, pH 7.5, 10% acetonitrile and buffer B: 100 mM Tris HCl, pH 7.5, 10% acetonitrile, 1 M NaCl) at a flow rate of 1.0 mL/min over 30 min, monitored at 260 nm.

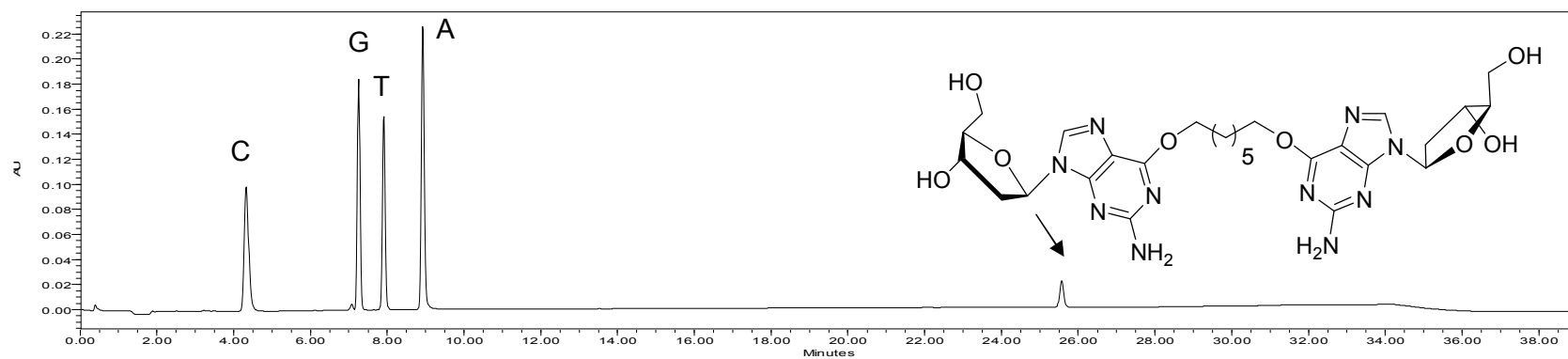


Supplementary Figure 7 - C-18 HPLC profile of digested cross-linked duplex **XL4** (A) and **XL7** (B). The column was eluted with a linear gradient of 0-60% buffer B over 30 min (buffer A: 50 mM sodium phosphate, pH 5.8 and buffer B: 50 mM sodium phosphate, pH 5.8, 50% acetonitrile) at a flow rate of 1.0 mL/min over 30 min, monitored at 260 nm.

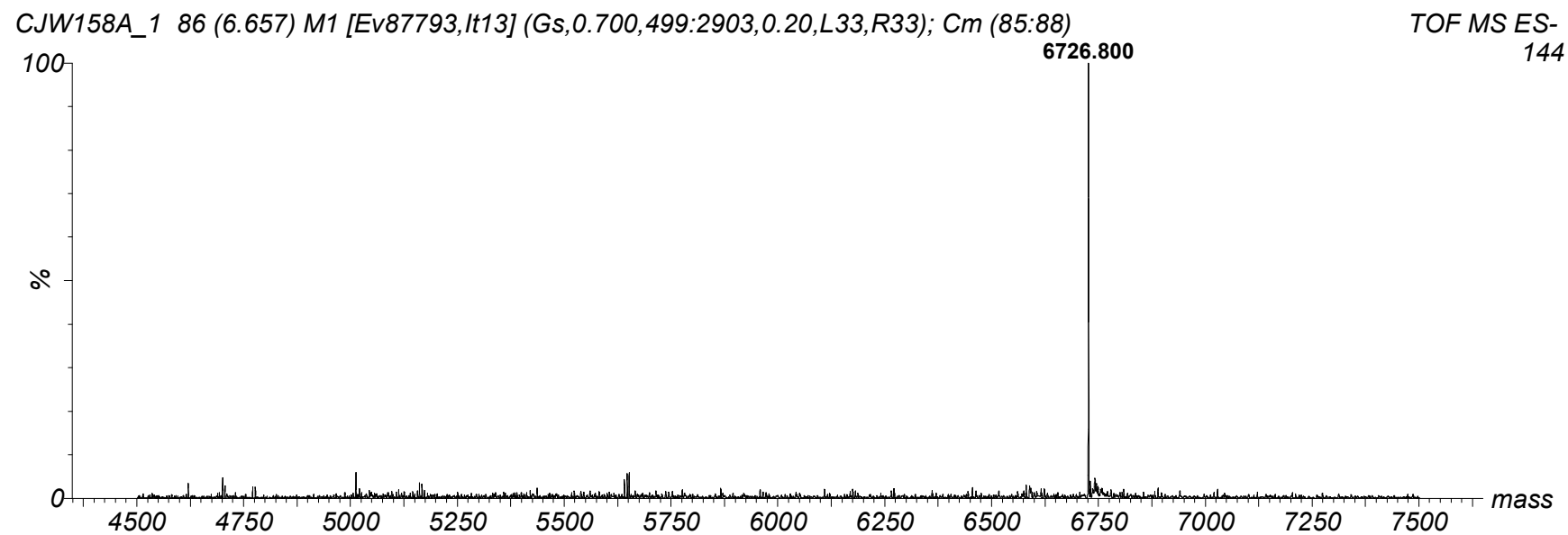
(A)



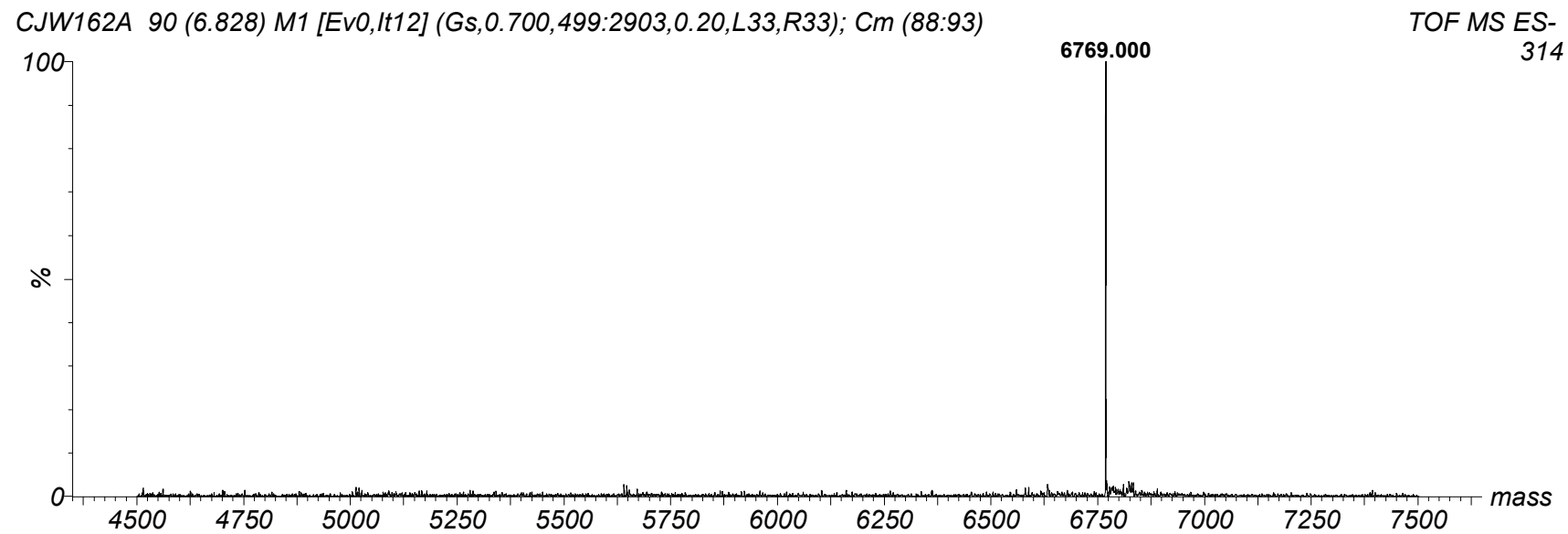
(B)



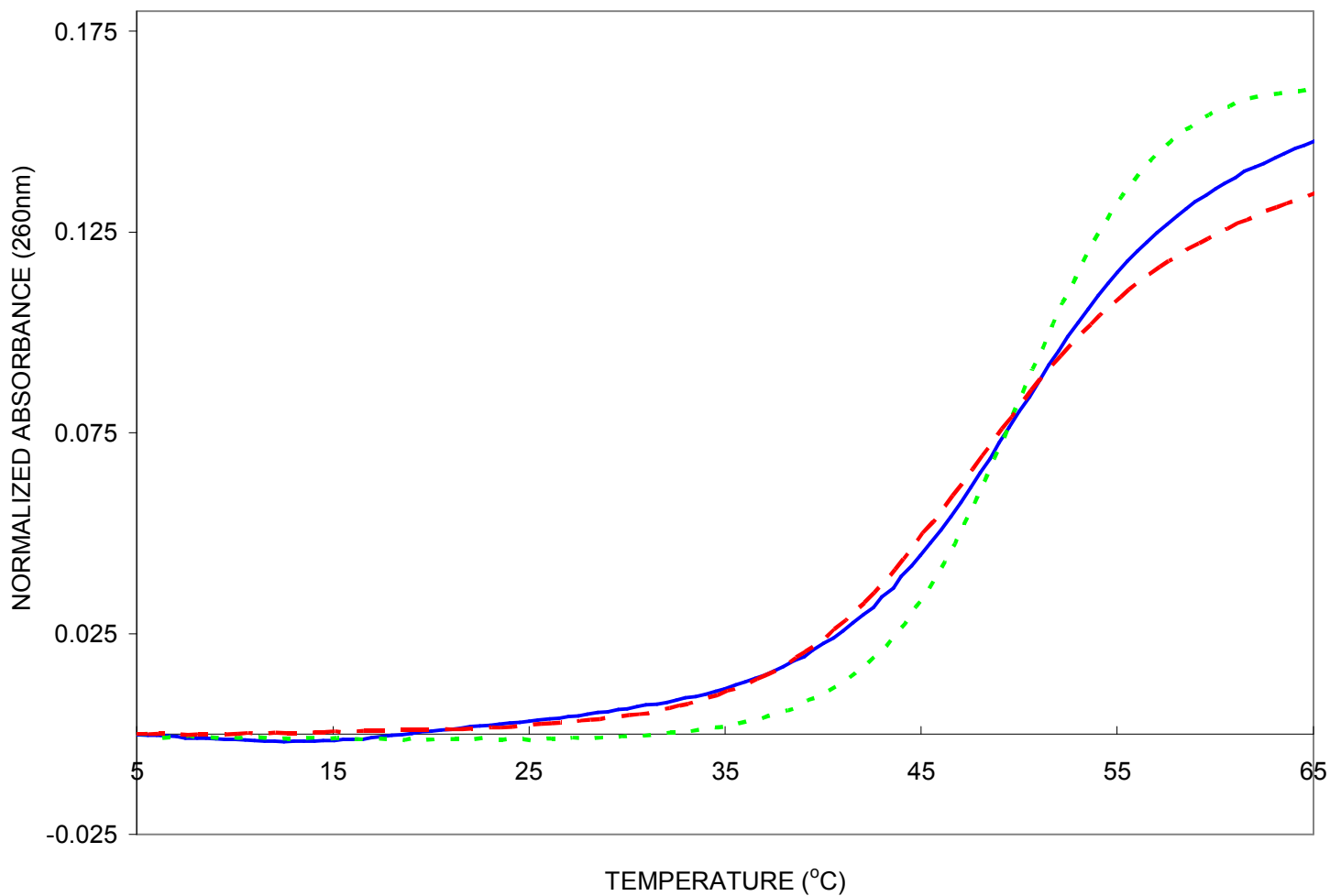
Supplementary Figure 8 - ESI MS spectrum of oligonucleotide **XL4**



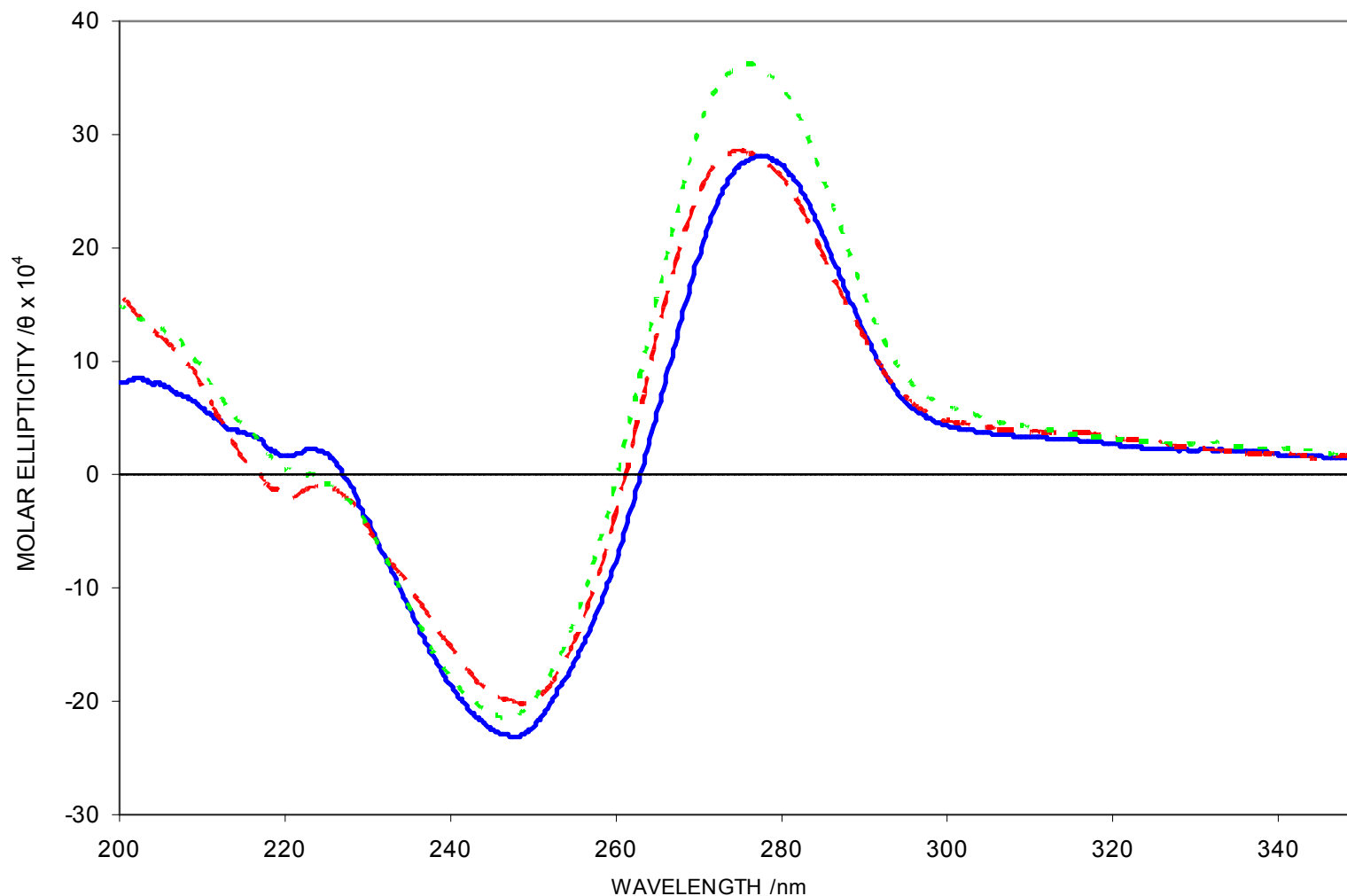
Supplementary Figure 9 - ESI MS spectrum of oligonucleotide **XL7**



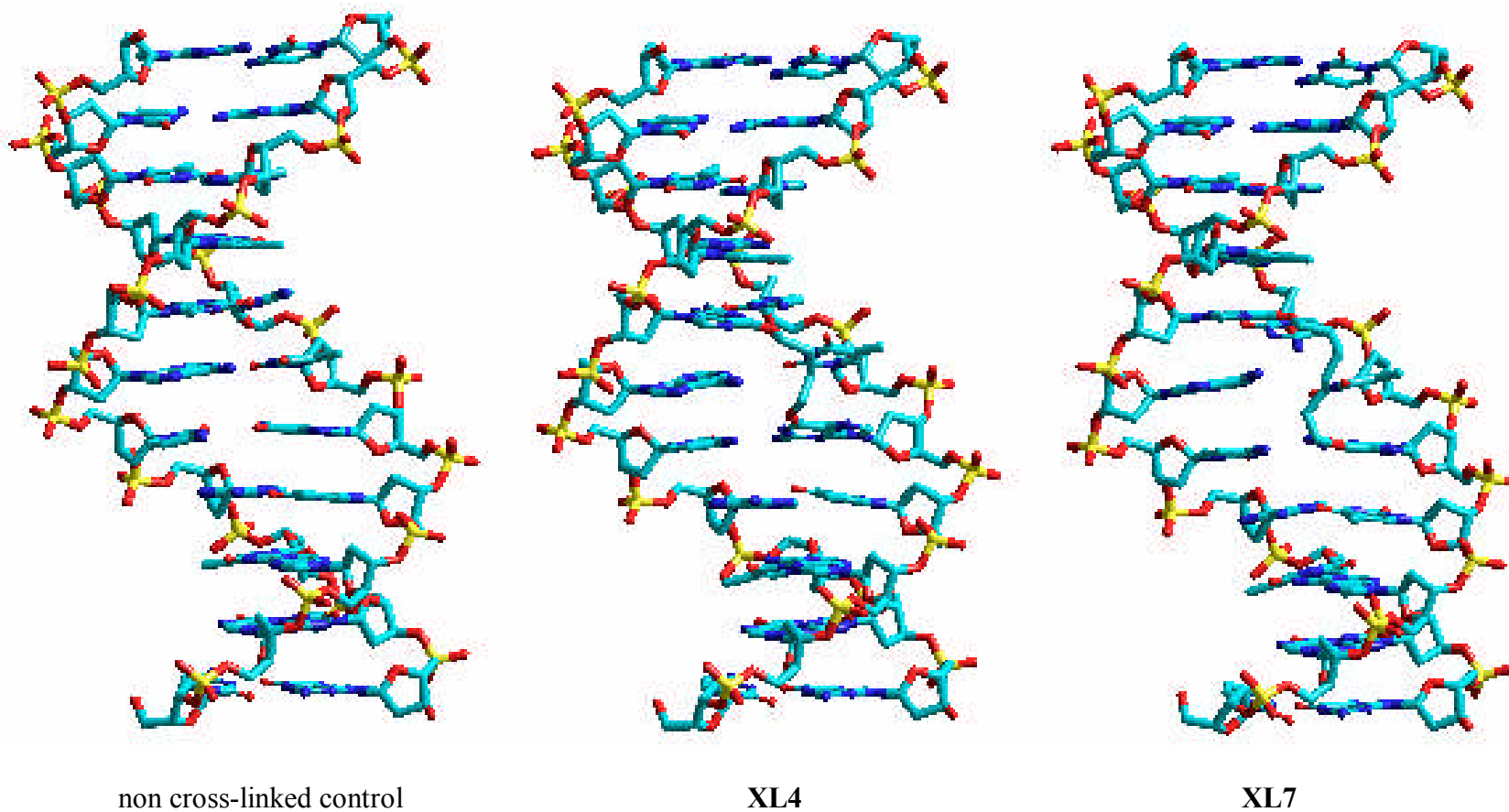
Supplementary Figure 10 - Absorbance (A_{260}) versus temperature profiles of non cross-linked duplex (____) 5'-dCGATGTCATCG-3'/5'-dCGATGACATCG-3', cross-linked duplex **XL4** (____), and cross-linked duplex **XL7** (.....). Solutions containing a total strand concentration of 2.8 μM for the cross-linked (**XL4** and **XL7**) and non-cross-linked control duplexes in 90 mM sodium chloride, pH = 7.0, 10 mM sodium phosphate, and 1 mM EDTA buffer, were heated at 0.5°C/min.



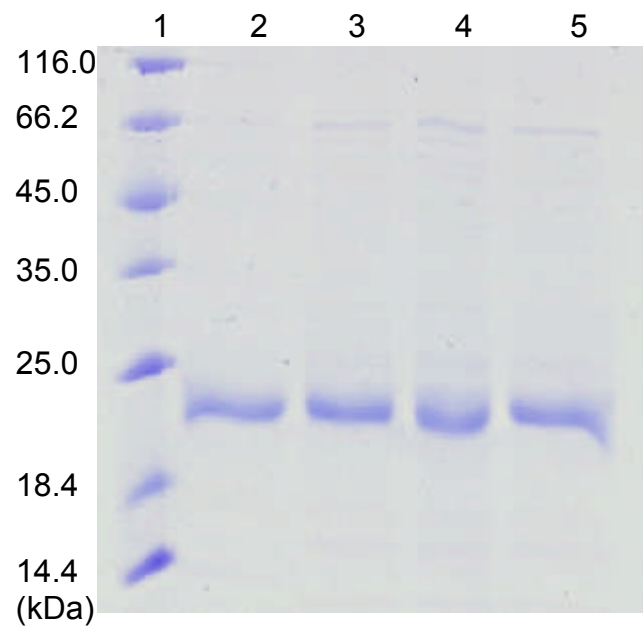
Supplementary Figure 11 - Circular dichroism spectra of non cross-linked duplex (____) 5'- dCGATGTCATCG-3'/5'-dCGATGACATCG3', cross-linked duplex **XL 4** (____), and cross-linked duplex **XL 7** (.....). Solutions containing a total strand concentration of 2.8 μM for the cross-linked duplex **XL 4,7** and 2.8 μM of the non-crosslinked control duplexes in 10 mM sodium phosphate, pH 7.0, 90 mM sodium chloride, and 1 mM EDTA. Spectra are the average of 5 scans and were recorded at 10 $^{\circ}\text{C}$.



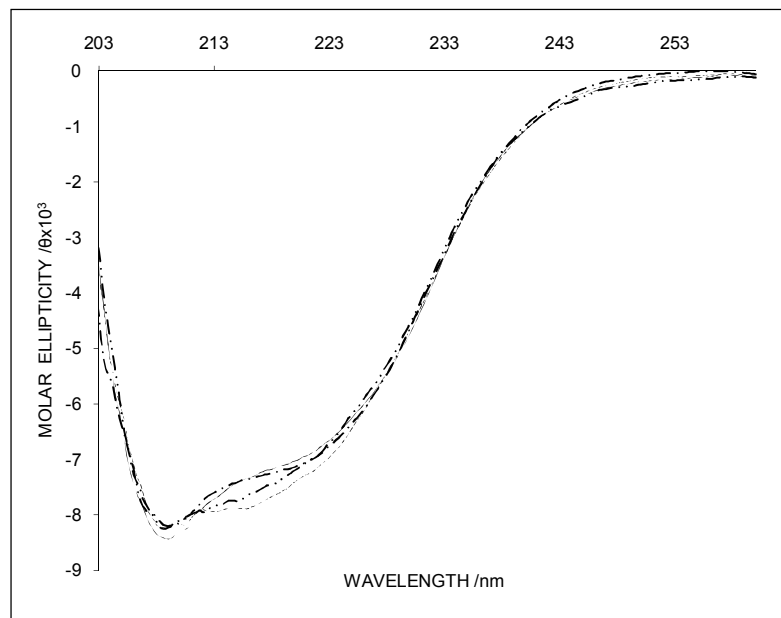
Supplementary Figure 12 – Molecular models of non cross-linked control duplex and cross-linked duplexes **XL4** and **XL7** that were geometry optimized using the AMBER forcefield.



Supplementary Figure 13 - 12% SDS-PAGE Gel of purified hAGT proteins. Loaded: lane 1, 10 μ L of Unstained Protein Molecular Weight Marker (Fermentas); lane 2, 7 μ g wild-type hAGT protein; lane 3, 7 μ g C145S hAGT protein; lane 4, 7 μ g P140A hAGT protein; lane 5, 7 μ g V148L hAGT protein.

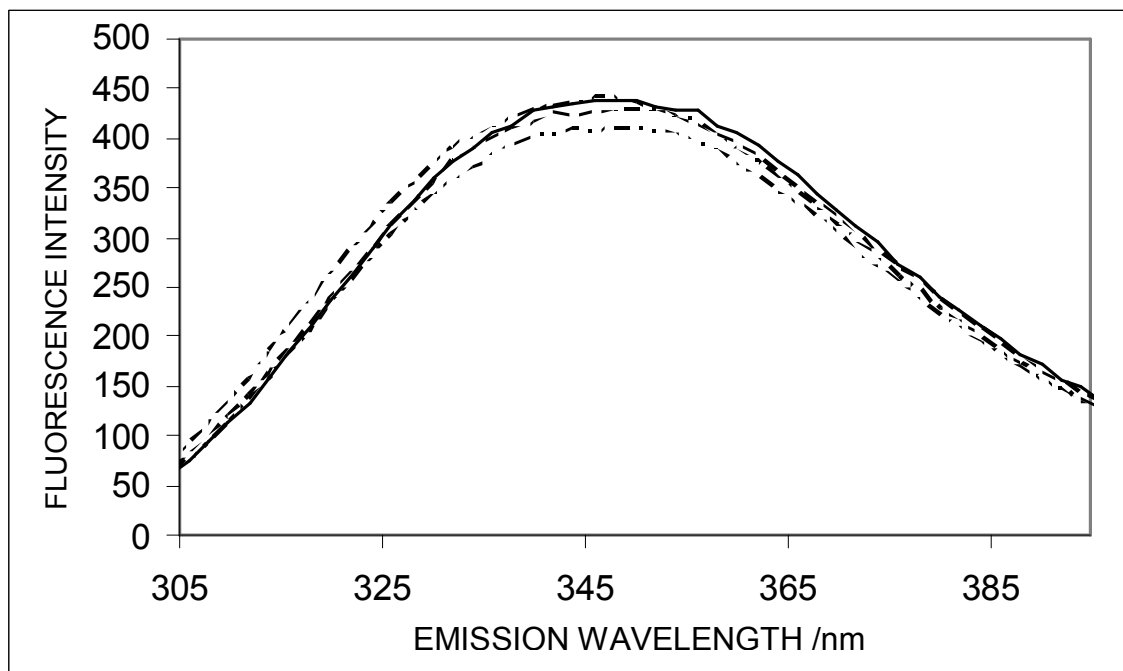


Supplementary Figure 14 - Effects of mutations on secondary structure of hAGT by circular dichroism. Scans were taken with 5 μ M wild-type hAGT (____), C145S (____), P140A (____) and V148L (____) between 260 and 200 nm in CD buffer (260-203 nm shown due to high voltage below 203nm).

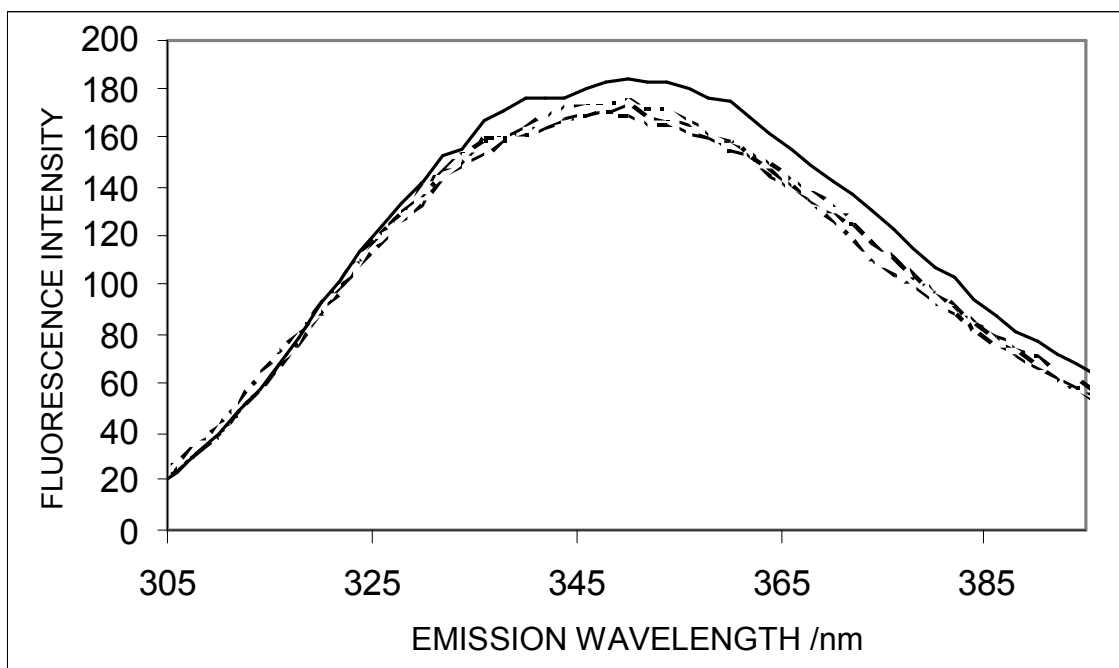


Supplementary Figure 15 - Effects of mutations on tertiary structure of hAGT by studying the intrinsic fluorescence signals of 1 μ M of wild-type hAGT (____), C145S (____), P140A (____) and V148L (____). **(A)** Monitoring of intrinsic tryptophan and tyrosine fluorescence. **(B)** Monitoring of intrinsic tryptophan fluorescence.

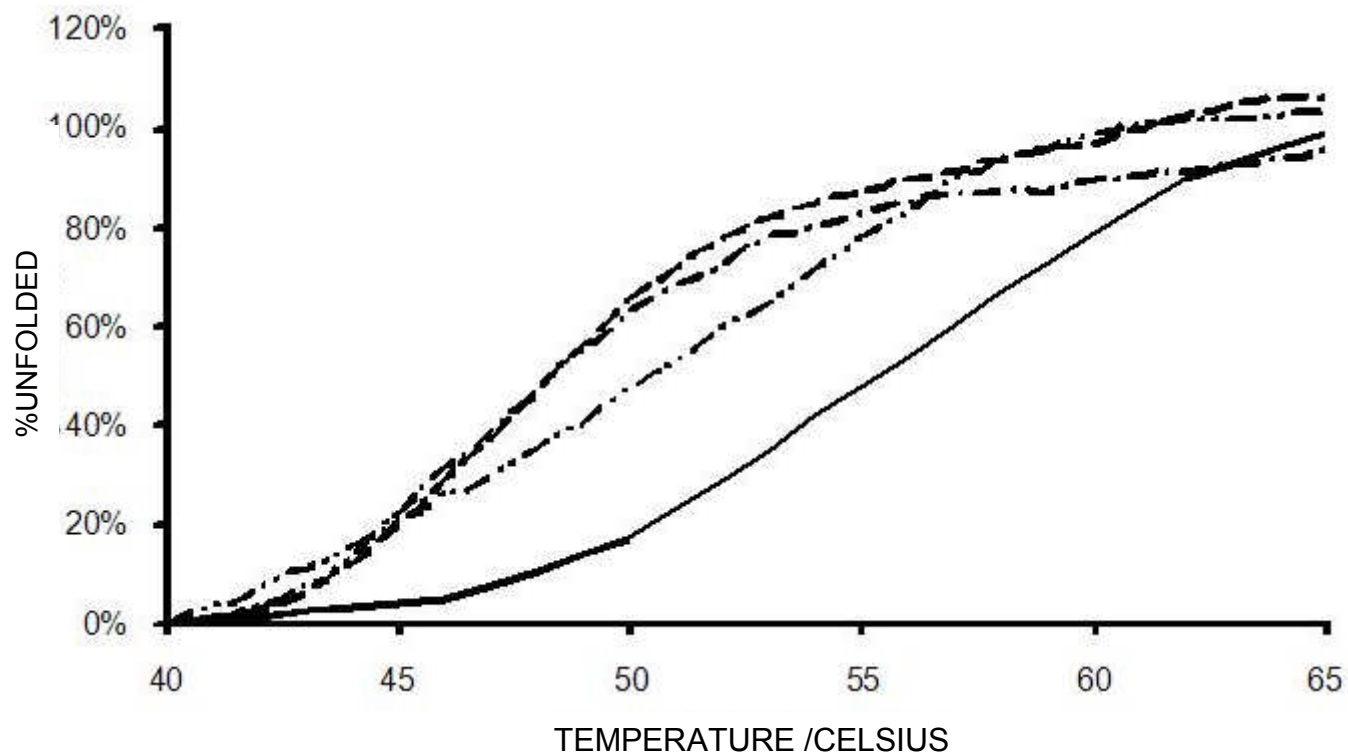
(A)



(B)

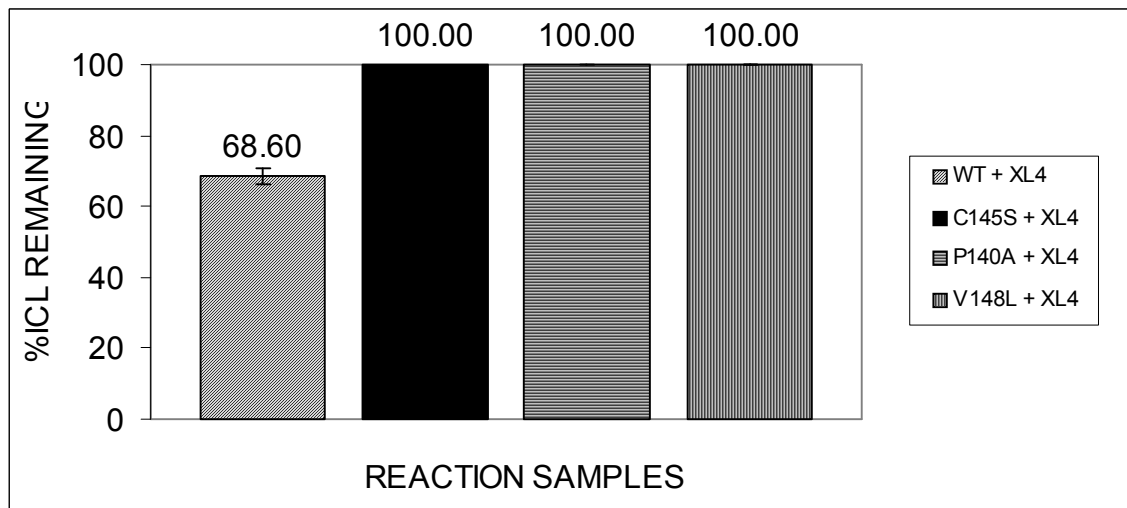


Supplementary Figure 16 - Effect of mutations on protein stability by thermal denaturation of 5 μ M wild-type hAGT (____), C145S (____), P140A (____) and V148L (____) by monitoring the change in molar ellipticity at 222nm.

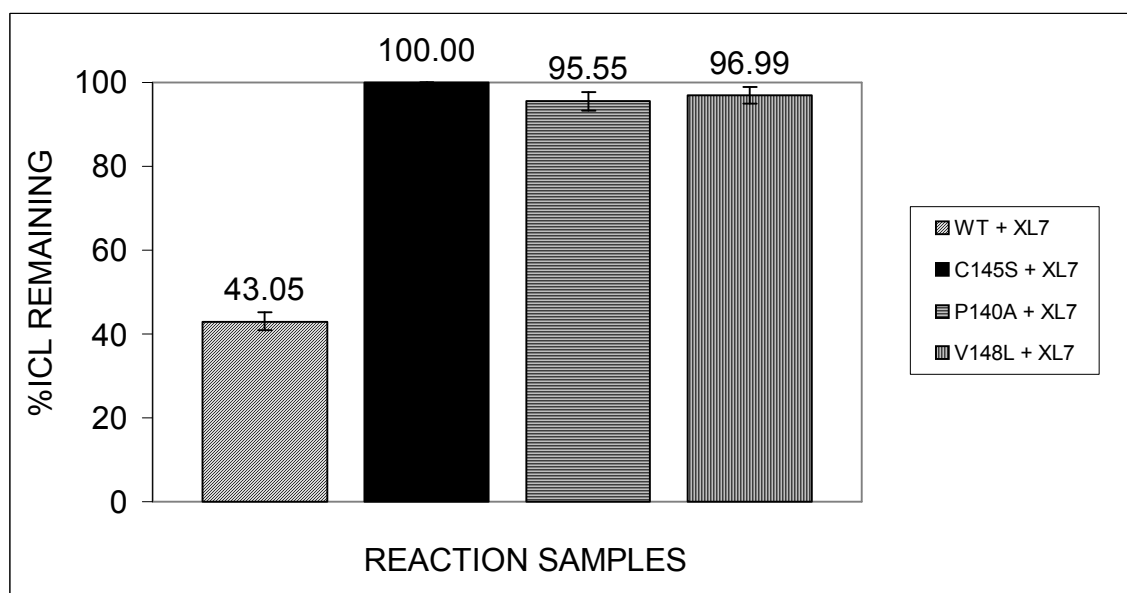


Supplementary Figure 17 – Graphic representation of the % ICL of (A) **XL4** and (B) **XL7** remaining in the reaction tube obtained using ImageQuant™.

(A)

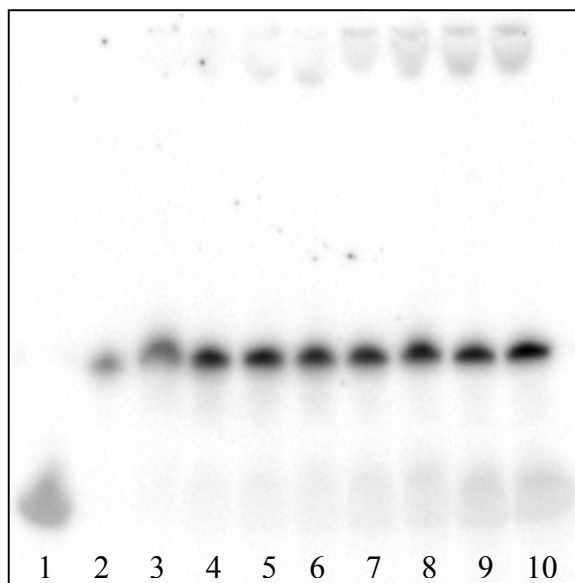


(B)

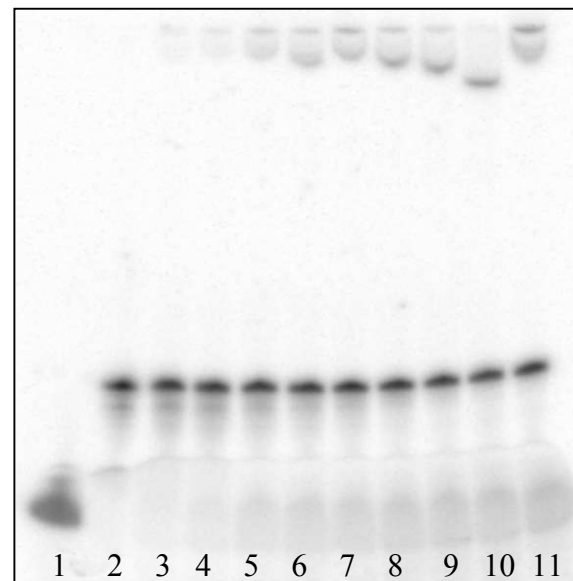


Supplementary Figure 18 – Time course repair of **XL4** and **XL7** by hAGT. **(A)** Denaturing gel of the repair of 2 pmol of **XL4** by 60 pmol hAGT as a function of time: lane 1, 2 pmol Control; lanes 2-10, 2 pmol **XL4** + 60 pmol hAGT incubated for 0, 5, 15, 30, 60, 120, 240, 510 and 540 min, respectively **(B)** Denaturing gel of the repair of 2 pmol of **XL7** by 60 pmol hAGT as a function of time: lane 1, 2 pmol Control; lanes 2-10, 2 pmol **XL7** + 60 pmol hAGT incubated for 0, 1, 2, 5, 10, 15, 30, 60, 120 and 180 min, respectively.

(A)

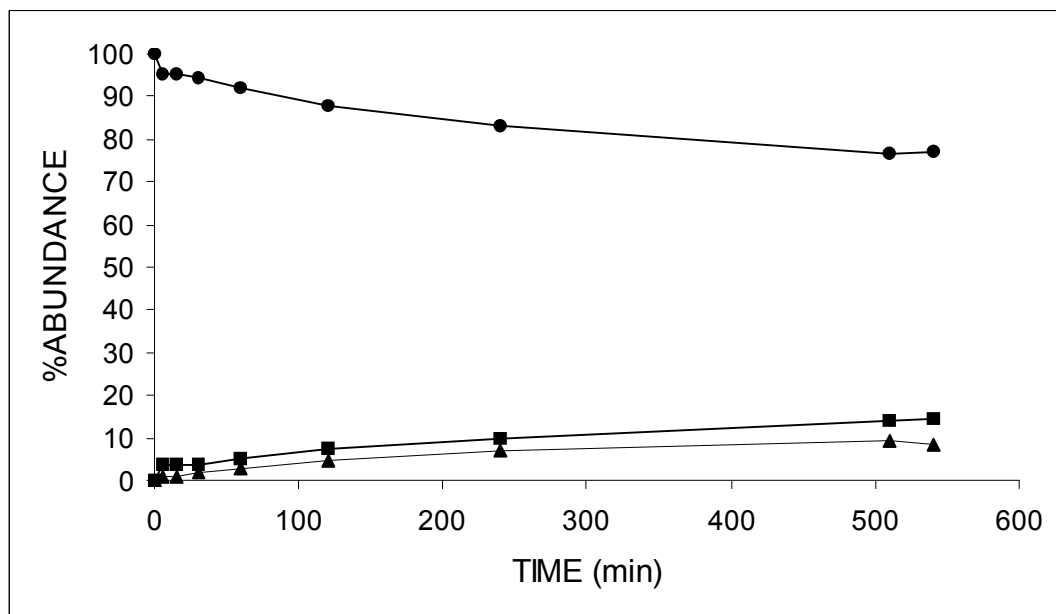


(B)

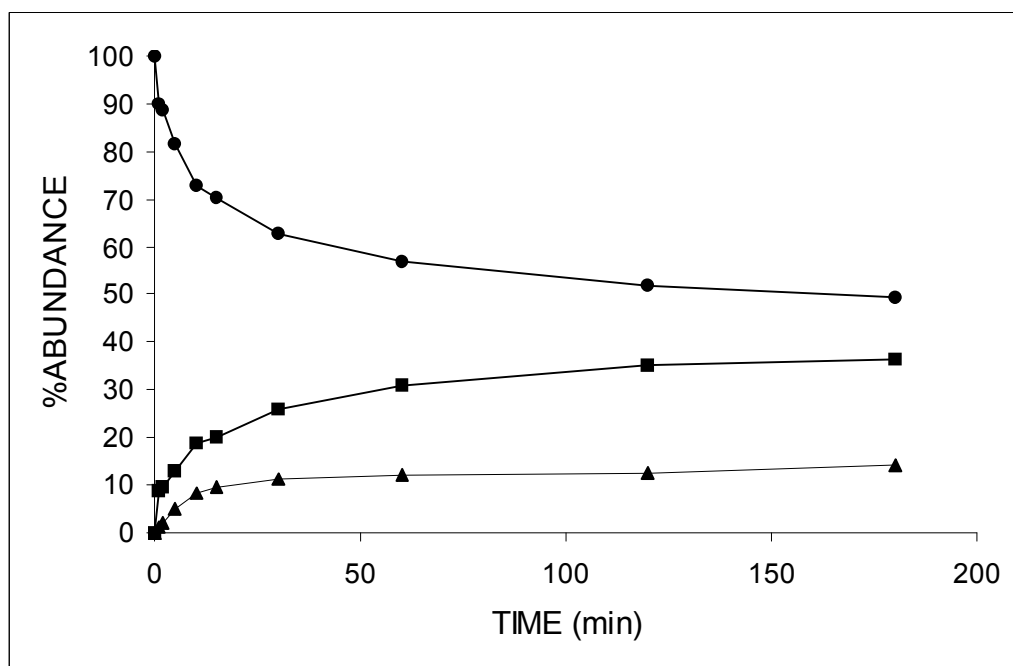


Supplementary Figure 19 – Graphic representation of the % abundance of each species in the time course repair by hAGT of (A) **XL4** and (B) **XL7** (see Supporting Information for denaturing gels). hAGT-DNA complex/partially repaired product (\blacktriangle); free DNA/ fully repaired product (\blacksquare); ICL/ unrepaired substrate (\bullet).

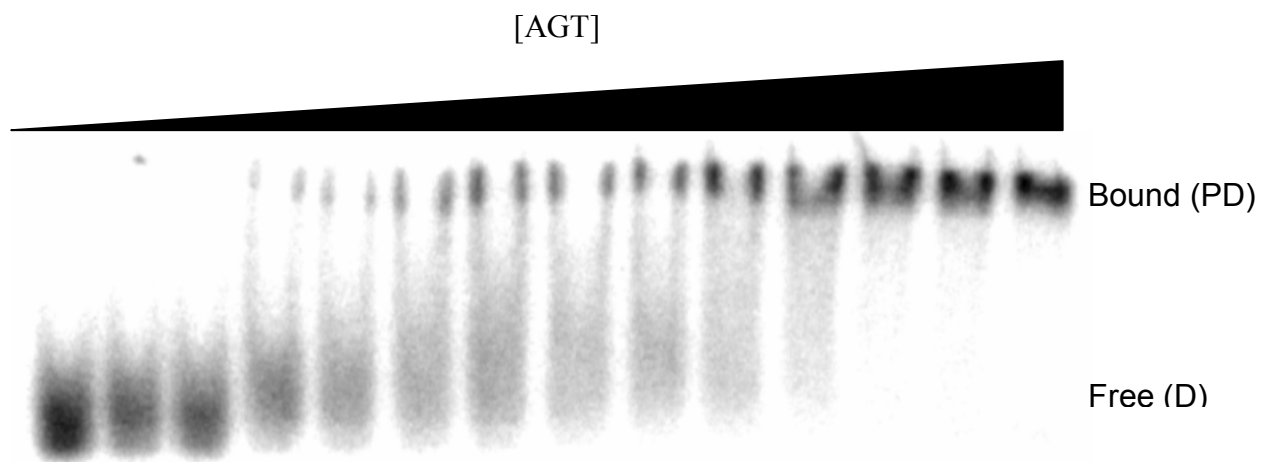
(A)



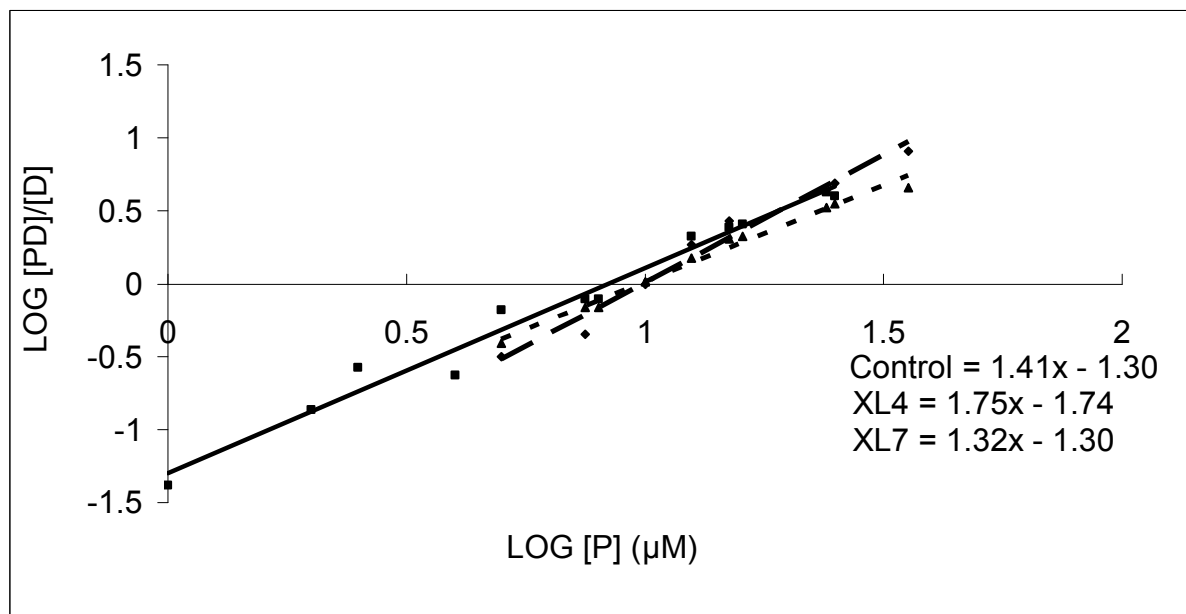
(B)



Supplementary Figure 20 - Electromobility shift assay of C145S hAGT binding to the control DNA duplex. EMSA Gel of C145S hAGT and the control 11-mer DNA duplex. 5 nM control DNA and 0 - 35.69 μ M C145S hAGT.



Supplementary Figure 21 - Hill plot representation of $\log[\text{PD}]/[\text{D}]$ versus $\log[\text{P}]$ for the control duplex (■), XL4 (◆) and XL7 (▲).



Supplementary Table 1 - ESI-MS results of wild-type hAGT and variants

Protein	Molecular Weight (Da)	
	Calculated	Observed
Wild-Type hAGT	21876.2	21875.0
C145S	21860.1	21860.0
P140A	21850.1	21850.5
V148L	21890.2	21889.5

Supplementary Table 2 – Effect of mutations on fluorescence emission signals of intrinsic hAGT on Tryptophan and Tyrosine (λ_{ex} 280nm) and Tryptophan only (λ_{ex} 295nm).

Protein	λ_{ex} 280nm		λ_{ex} 295nm	
	λ_{em} (nm)	Fluorescence Intensity	λ_{em} (nm)	Fluorescence Intensity
Wild-Type hAGT	346	438	350	184
C145S	350	409	350	176
P140A	346	440	348	169
V148L	350	428	350	173

Supplementary Table 3 - Difference in T_m between mutants and wild-type hAGT.

Protein	Melting Temperature (°C)		
	Observed	Wild-Type	Difference
Wild-Type hAGT	56.5	56.5	0.0
C145S	50.7	56.5	-5.8
P140A	47.0	56.5	-9.5
V148L	48.0	56.5	-8.5